Journal of Metals, Materials and Minerals, Vol. 31, No. 3, pp. 10-19, 2021

Extraction of cellulose nanofibers from empty palm fruit bunches via mechanical defibrillation

Zi-Qian TAN[1,2], Takaomi KOBAYASHI[2], and Duangdao AHT-ONG[1,3,*]

[1] *Department of Materials Science, Faculty of Science, Chulalongkorn University, Bangkok 10330, Thailand*
[2] *Department of Materials Science and Technology, Nagaoka University of Technology, 1603-1 Kamitomioka, Nagaoka, Niigata 940-2188, Japan*
[3] *Centre of Excellence on Petrochemical and Materials Technology, Chulalongkorn University, Bangkok 10330, Thailand*

***Corresponding author e-mail:** duangdao.a@chula.ac.th

Received date:
7 May 2021
Revised date
18 August 2021
Accepted date:
22 August 2021

Keywords:
Cellulose nanofibers;
Empty palm fruit bunches;
Mechanical defibrillation;
High-pressure homogenization

Abstract

In recent years, there has been an increasing interest in finding alternative material to replace fossil-oil based product due to the environmental concern. Lignocellulosic biomass has emerged as the promising candidate due to its low-cost and sustainability. The objective of this work was to prepare cellulose nanofibers (CNFs) from empty palm fruit bunches (EPFB), which are the waste originating from palm oil industry. Cellulose fibers were first extracted from EPFB by chemical treatment, followed by mechanical disintegration using high-pressure homogenization. Fiber concentration and defibrillation time during mechanical treatment were studied to investigate their effects on the properties of produced nanofibers. The obtained micro- and nano-fibers were characterized using Fourier transform infrared spectroscopy (FTIR), X-ray diffractometer (XRD), Thermogravimetric analyzer (TGA), Scanning electron microscope (SEM) and Transmission electron microscope (TEM). The results indicated that non-cellulosic components were successfully removed by chemical treatment, as evidenced by the disappearance of lignin and hemicellulose related peaks in FTIR analysis, reduction of their content in chemical composition result, and increase in the thermal stability for purified fibers. Moreover, TEM images and diameter distribution analysis revealed that fiber concentration of 0.5%w/v provided the best diameter size uniformity with the nanofiber's diameter ranged 6 nm to16 nm, as compared to higher fiber concentration.

1. Introduction

Synthetic polymers with highly tailorable characteristics and a wide range of application have been manufactured to fulfill human needs. However, these synthetic polymers are heavily relying in fossil resources. Considering their non-biodegradable characteristics and environmental impacts, such as global warming and waste issues, there is a need to put greater efforts for finding sustainable materials based on natural resources [1]. The major component of lignocellulosic biomass, cellulose, has been extensively highlighted due to its unique properties including renewability, good biocompatibility, outstanding mechanical properties, and customizable surface chemistry [2]. With the selection of proper chemical, mechanical, or enzymatic methods, cellulose size can be reduced into nanoscale. By doing so, some of the imperative characteristics of cellulose-based materials such as functionality, uniformity and durability can be improved. For instance, nanoform of cellulose exhibits enhanced mechanical properties due to their high surface-to-volume ratio and aspect ratio [3].

The term 'Nanocellulose' has been introduced and refers to cellulose materials having at least one dimension in nanometer range. There are three main types of nanocellulose, which are cellulose nanofibers (CNF), cellulose nanocrystals (CNC), and bacterial cellulose (BC), with different dimensions, functions, and preparation method [3]. In view of lignocellulosic biomass as the source for cellulose, BC is not discussed herein. CNCs can be produced via acid hydrolysis of the amorphous section of cellulose fibers while the preparation of CNFs is much simpler as it can be prepared by physical separation of cellulose fibers, such as grinding, high-pressure homogenization, and ultrasonication, without severe chemical cleavage on cellulose chain molecular structure [4].

Empty palm fruit bunches (EPFB), one type of biomass waste originated from palm oil industry have been considered as a suitable source for CNFs extraction due to its wide availability and abundance. At a yearly basis, more than 12.4 million tons and 3.8 million tons of EPFB can be generated in Malaysia and Thailand, respectively [5,6]. In addition, as compared to other oil palm biomass such as oil palm fronds, oil palm trunks and palm kernel shells, EPFB consists of higher amount of cellulose, up to 38.7% [7]. Several mechanical treatments were applied to isolate CNFs from EPFB including nano-grinding, high pressure homogenization and steam explosion [8-12]. In high-pressure homogenization, purified fibers are used as the starting materials. By exposing the fibers to rapid pressure drops, high shear, and impact forces against homogenization valve and an impact ring, CNFs are obtained [13]. However, to the best of our knowledge, no study has been carried out to investigate the effect of fiber concentration and defibrillation time on the properties of CNFs extracted from EPFB.

Therefore, in this paper, the effect of high-pressure homogenization parameters on the properties of CNFs in terms of chemical composition, thermal stability, morphology, and crystalline structure were investigated.

2. Experimental procedure

2.1 Materials preparation

EPFB were obtained from southern area of Thailand and dried under sunlight. Then, they were cut and washed with water several times to remove the soil and impurities. To remove moisture, they were dried in oven at 60°C for at least 24 h until constant weight. Prior to chemical treatments, dried EPFB were ground into micro size and passed through 0.2 mm opening sieve. The chemical used in this experiment, sodium hydroxide (NaOH) and sodium chlorite ($NaClO_2$) were purchased from NT Chemical (Bangkok, Thailand) while glacial acetic acid (CH_3COOH) was supplied by Ajax Finechem. All chemicals were of analytical grade.

2.2 Chemical treatment

The raw fibers were treated using 5%w/v NaOH solution at 80°C under continuous stirring for 2.5 h. After that, they were filtered and washed with deionized water until the pH reached neutral. The alkali-treated fibers were then treated with 5%w/v $NaClO_2$ solution, with pH adjusted to 3.5 by CH_3COOH solution. The mixture was stirred continuously at 80˚C for 2 h, followed by filtering and washing with deionized water until pH reached neutral. The entire alkali treatment and bleaching procedure were repeated 2 times and 3 times, respectively. Both alkali treatment and bleaching processes were adapted from the study reported elsewhere [12,14].

2.3 Isolation of cellulose nanofibers

The purified fibers were dispersed in deionized water and mechanically treated using high-speed blender (BUO-121280, BUONO, Taiwan) at a speed of 38,000 rpm for 5 min. Various fiber concentrations were prepared at 0.5, 0.7, and 1.0 % w/v. After that, the suspensions were passed through a high-pressure homogenizer (M-110P, Microfluidics, Westwood, MA) at 20,000 psi. The connected cooling system was controlled at 12°C to 15°C to prevent overheating. The defibrillation time was monitored at 30 min and 60 min for each fiber concentration to study the effect of defibrillation time on the characteristics of the CNFs.

2.4 Characterization

The yield of purified fibers obtained after chemical treatment was determined based on gravimetric analysis. Before measurements, samples were oven-dried at 60°C to remove moisture. Chemical composition of cellulosic fibers were determined according to the method described by Goering and Van Soest [15]. Briefly, cellulose content was determined by the difference between acid-detergent fiber (ADF) and amount of lignin while hemicellulose content was calculated by the difference between neutral-detergent fiber (NDF) and acid-detergent fiber (ADF).

Fourier transform infrared (FTIR) measurements were performed using a spectrometer (Nicolet iS50, Thermo Fisher Scientific, Waltham, MA) with transmission mode, by pellet preparation with KBr. The raw fibers, purified fibers and CNFs were analysed at wavenumbers of 400 cm^{-1} to 4000 cm^{-1} with 4 cm^{-1} resolution and 32 repetitious scans. Prior to the measurement, the background spectrum was recorded.

The morphology of the dried fibers were examined by a scanning electron microscope (SEM, JSM-6610LV, JEOL Ltd., Tokyo, Japan) and a field emission scanning electron microscope (FE-SEM, Hitachi SU8030, Hitachi High-Tech Co, Tokyo, Japan), operated at 10kV and 3kV of acceleration voltage, respectively. Prior to the analysis, the samples were fixed on aluminium stubs with double-sided tape and sputter-coated with a gold layer. The defibrillation mechanism of CNFs after defibrillation were also studied by a transmission electron microscope (TEM, JEM-1400, JEOL Ltd., Tokyo, Japan). Approximately 10 µL of diluted CNFs suspension was dropped on a carbon coated copper grid, then the grids were negatively stained with 1%w/v uranyl acetate for 5 min and dried at room temperature. Each sample was investigated at 80 kV of accelerating voltage. By using ImageJ software, the diameter of raw fibers, purified fibers and CNFs was measured from SEM and TEM micrographs. Diameter distribution analysis was performed for CNFs and the mean values, standard deviations and variation ranges were calculated. For each sample, 25 fibers were randomly selected and measured from TEM images.

The optical transmittance of CNFs suspensions was measured using a UV-Vis Spectrophotometer (UV 9100 – Series, LabTech, Hopkinton, MA). Briefly, a diluted dispersion of CNF in water at 0.1%w/v was prepared and the transmittance was measured from 400 nm to 700 nm. The spectrum of a cuvette filled with water was used as a reference.

Thermal stability of raw fibers, purified fibers and CNFs were investigated by a thermogravimetric analyser (TGA/DSC 3+ LF, Mettler Toledo, Greifensee, Switzerland). In brief, 2 mg to 5 mg of each sample was placed into a 70 µL alumina crucible and heated from 50°C to 600°C with a heating rate of 10°C·min^{-1} and the flow rate of N_2 was 20 mL·min^{-1}.

Degree of crytallinity of raw fibers, purified fibers and CNFs were analysed using an X-ray diffractometer (XRD, D8 Advance, Bruker, Karlsruhe, Germany), with Cu-Kα radiation at 40 mA and 40 kV. Scattered radiation was recorded in the interval $5° \leq 2\theta \leq 50°$. The crystallinity index (CI) was estimated using equation (1), according to Segal *et al*. [16].

$$CI\ (\%) = \frac{I_{002}-I_{am}}{I_{002}} \times 100 \quad (1)$$

Where I_{002} is the maximum diffraction intensity of the peak of 2θ between 21° and 23°; I_{am} is the diffraction intensity of the amorphous material, in which 2θ is located between 18° and 20°, which is the minimum diffraction intensity for cellulose I.

3. Results and discussion

3.1 Chemical composition and yield analysis

The composition of cellulose, hemicellulose and lignin in lignocellulosic biomass varies depending on the type of biomass, species of the plant, and the sources of the biomass [17]. Table 1 shows the chemical composition of the raw fibers and purified fibers of EPFB. Raw fibers consisted of 57.63% cellulose, 17.61% hemicellulose, 8.34% lignin, and 0.04% ash. After chemical treatment, the amount of hemicellulose and lignin decreased significantly, making the purified fibers to contain high cellulose content of 88.14%. The reduction of lignin and hemicellulose was due to their solubilization during chemical treatment, without degrading cellulose. The ester-linked substituents of the hemicelluloses were broken, as well as ester-linked phenolic monomers such as ferulic acid (FA), ρ-coumaric acid and sinapic acid [18].

The yield of bleached fibers as compared to raw fibers was approximately 36%, owing to the removal of hemicellulose, lignin, and other extractives. As clearly seen in Figure 1, raw fibers showed brownish colour contributed by the presence of non-cellulosic substance. After chemical treatments, the purified fibers turned into white colour due to the removal of such substances. For cellulose nanofibers, the structure became gel-like from watery after passing through high-pressure homogenization, while the colour was in white as well.

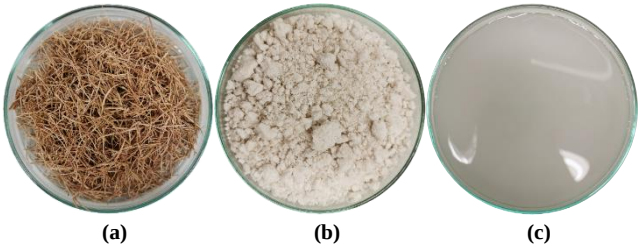

Figure 1. Appearance of (a) raw fibers, (b) purified fibers and (c) cellulose nanofibers suspension.

3.2 Fourier transform infrared spectroscopy

The FTIR spectra of raw fibers, purified fibers and CNFs are illustrated in Figure 2. Characteristic peaks of lignocellulosic materials were observed for all samples. The peaks at 3370 cm^{-1} and 2900 cm^{-1} were associated with the stretching vibration of the OH and CH groups exist in the cellulose chains [19-21]. For the purified fibers, there was no detection of peak intensity at 1734 cm^{-1} for carbonyl C=O stretching vibrations of acetyl and uronic ester groups, indicating the removal of hemicellulose and the ester linkage of the carboxylic group of ferulic and ρ-coumaric acids of lignin or hemicellulose contained in the raw fibers [22]. The bands around 1590 cm^{-1} and 1490 cm^{-1} as seen in the raw fibers, represented the C=C vibration of aromatic ring in lignin. The peak at 1450 cm^{-1} was attributed to the symmetric bending of CH_2 [23]. Moreover, the peak at 1240 cm^{-1} was seen in raw fibers, indicating the presence of C-O bond, out of plane stretching vibration of aryl group in lignin [10]. All these mentioned peaks were reduced or nearly disappeared for purified fibers and CNFs, suggesting non-cellulosic components have been removed. In addition, the peak at 1060 cm^{-1} was the characteristic peak of anhydroglucose chains with a C-O stretch, while peak at 890 cm^{-1} was attributed to C-H stretching vibration of the alkyl group in the aliphatic chain of lignocellulosic fibers [24].

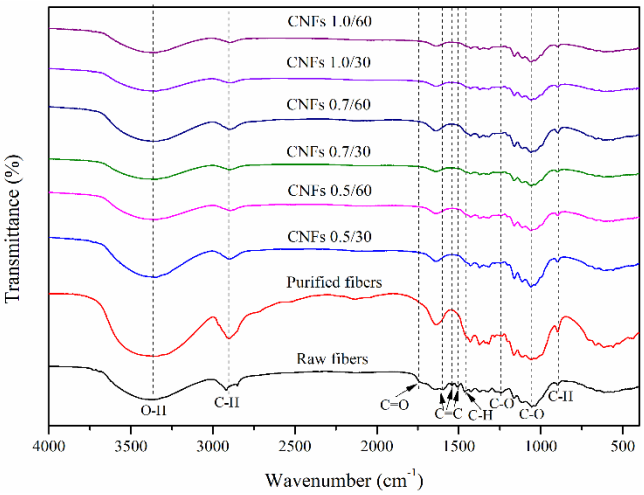

Figure 2. FTIR spectra of raw fibers, purified fibers and CNFs.

3.3 Morphological structure

The SEM micrographs of the raw fibers and purified fibers are shown in Figure 3. Raw fibers had a rough surface due to the presence of wax, oil, and starch granule components around the fibers bundle. After chemical treatment, the surface became smoother, indicating the removal of non-cellulosic components [25]. Furthermore, some pores were observed on the surface of purified fibers (Figure 3(d)). The similar phenomenon was also reported for bamboo fibers after alkali treatment [26]. This can be explained by the swelling of cellulose caused by alkali that disturbs the cross-links between hemicelluloses and lignin/cellulose and thereby improving the biomass porosity [27]. Comparing raw fibers and purified fibers at same magnification, reduction of size was seen. This was caused by the loosening of non-cellulosic components that hold the cellulose fibers and caused separation of fibers bundles into individual fibers. The diameter of raw fibers was in the range of 9.2 μm to 32.2 μm, while the diameter of purified fibers was narrowed down to 9.7 μm to 17.0 μm (Figure S1 and S2).

Table 1. Chemical composition of raw fibers and purified fibers.

Samples	Composition (%)			
	Cellulose	Hemicellulose	Lignin	Ash
Raw fibers	57.63 ± 0.68	17.61 ± 0.36	8.34 ± 0.62	0.04 ± 0.01
Purified fibers	88.14 ± 0.32	5.51 ± 0.35	0.60 ± 0.04	0.07 ± 0.01

Due to the limited magnification, FE-SEM was used to observe the morphology of CNFs. Figure 4 presents the FE-SEM micrographs of the CNFs prepared at various fiber concentrations and defibrillation time. It was found that increased fiber concentration tended to obtain CNFs with mixture of high and low fiber diameter. This finding suggested that at higher fiber concentration, nanofibers in the high-pressure homogenizer have lower chance to encounter mechanical attack, as compared to lower fiber concentration at 0.5%w/v. Meanwhile, at fiber concentration of 0.5%w/v, better uniformity of diameter size was achieved, as shown in Figure 4(a), indicating higher performance for size reduction.

Figure 5 shows the TEM images of CNFs prepared at various conditions while Figure 6 shows the fiber diameter distribution histogram. At the defibrillation time of 30 min, the distribution chart of 0.5%w/v fiber concentration shows that all CNFs were in the range of 6 nm to 16 nm, with the average diameter of 10.3 ± 2.7 nm (Figure 6(a)). The variation range was 9.4 nm (Table S3), indicating a narrow diameter distribution and good uniformity. For fiber concentration of 0.7 and 1.0%w/v, it can be noticed that majority of CNFs diameter lied between 10 nm to 20 nm and 5 nm to 10 nm, respectively (Figure 6(c) and 6(e)). However, some large fiber with diameter greater than 20 nm were seen, contributing to around 5% of the overall distribution. These results were well agreed with FE-SEM images that showed uniformity on the diameter size for 0.5%w/v fiber concentration, and presence of larger nanofibers for higher fiber concentration. The result showed that at defibrillation time of 30 min, low concentration at 0.5%w/v gave the best uniformity of fibers diameter, which is similar to that reported by Pacaphol and Aht-Ong [14].

In addition, when defibrillation time was prolonged from 30 min to 60 min, higher amount of fine fiber branches were observed, as shown in Figure 5(b), 5(d), and 5(f). This phenomenon was as well observed in the diameter distribution chart, whereby the diameter distribution for all fiber concentrations was dominated by smaller diameter fibers than that of 30 min of defibrillation time. This can be explained by the longer period that fibers experienced mechanical attack in high-pressure homogenizer as compared to shorter defibrillation time.

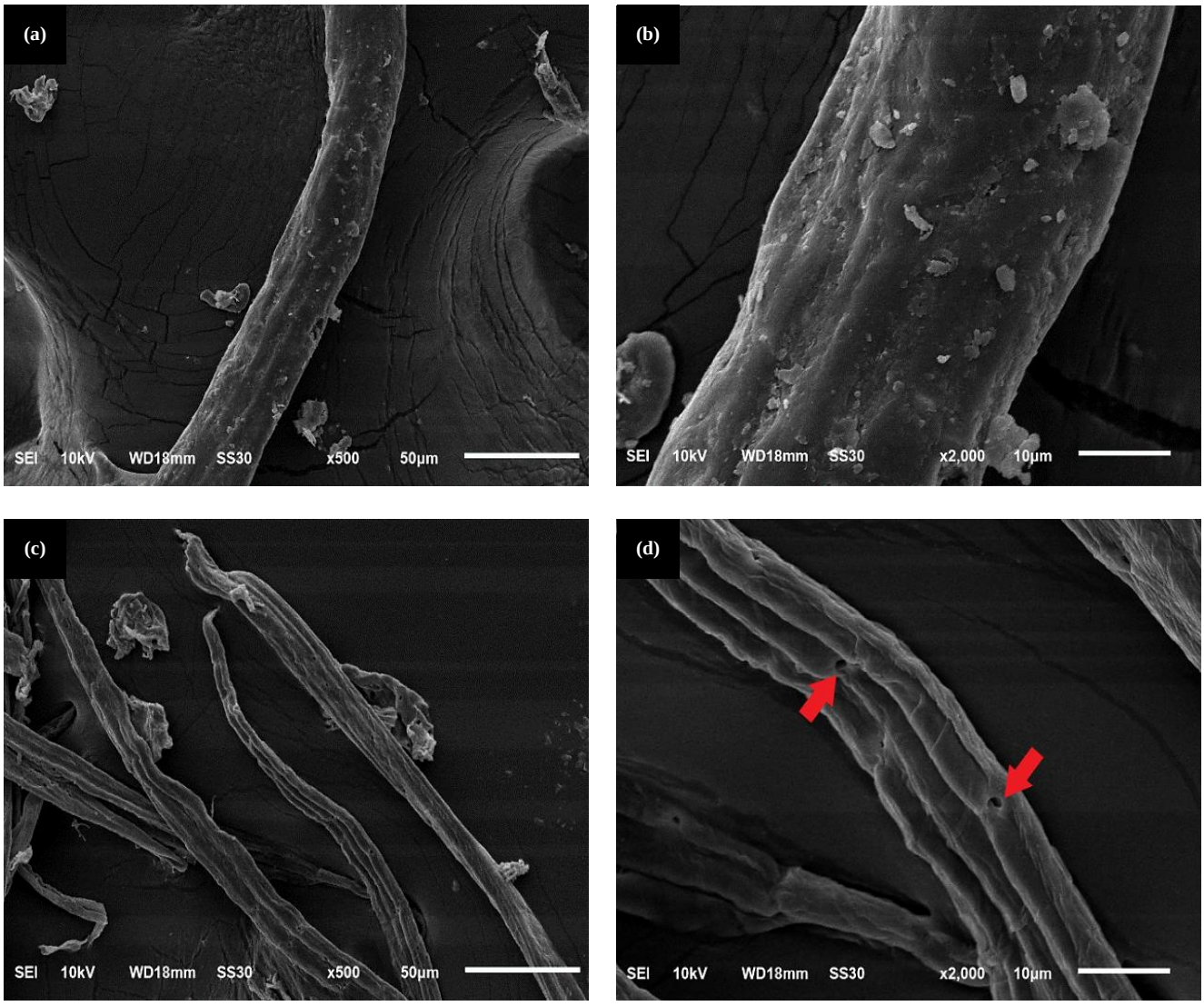

Figure 3. SEM micrographs of (a, b) raw fibers and (c, d) purified fibers at 500× and 2000× magnifications, respectively.

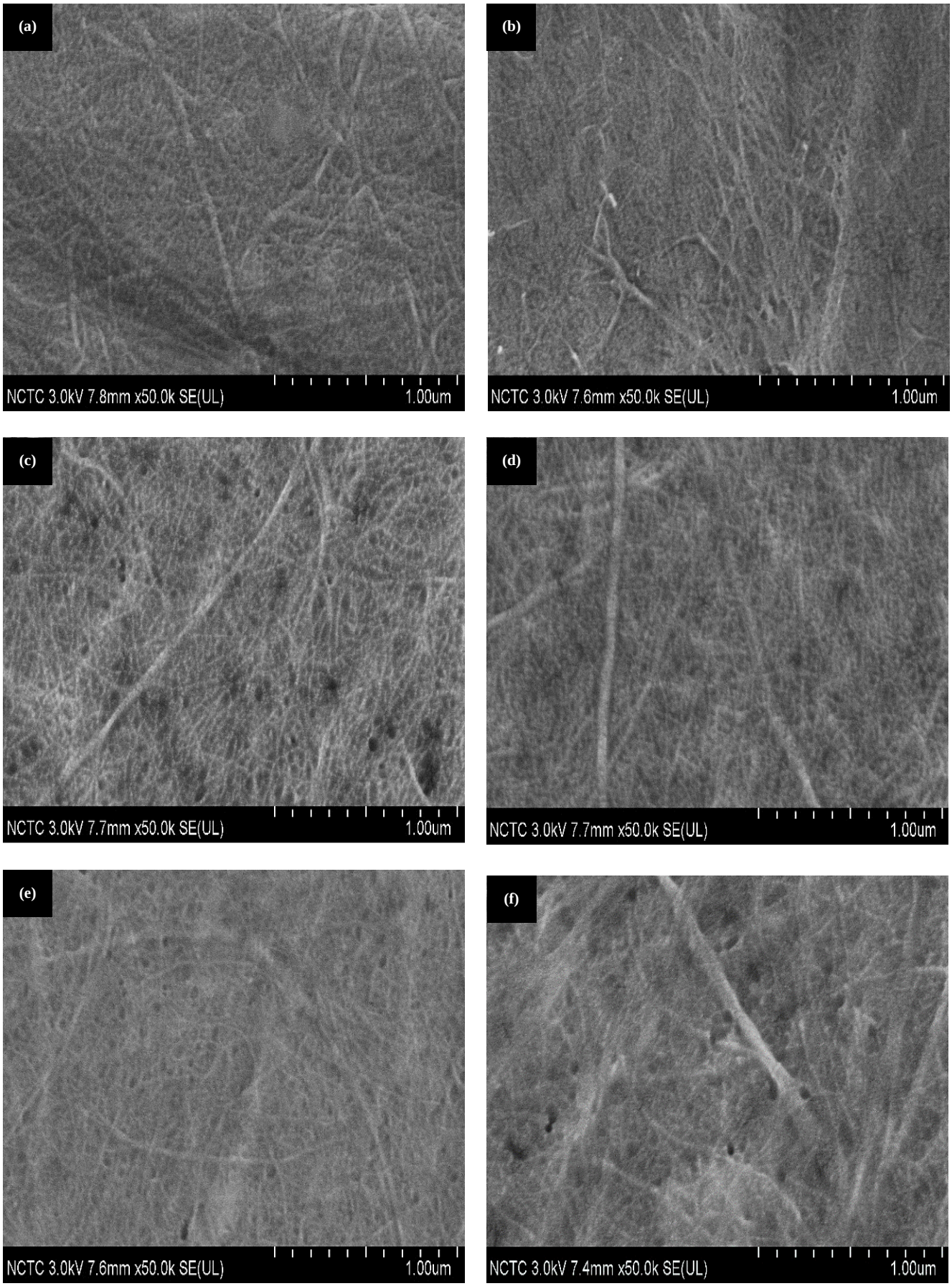

Figure 4. FE-SEM micrographs at 50,000× magnifications of the CNFs: (a, b) 0.5%, (c, d) 0.7% and (e, f) 1.0%, for defibrillation time of 30 min and 60 min, respectively.

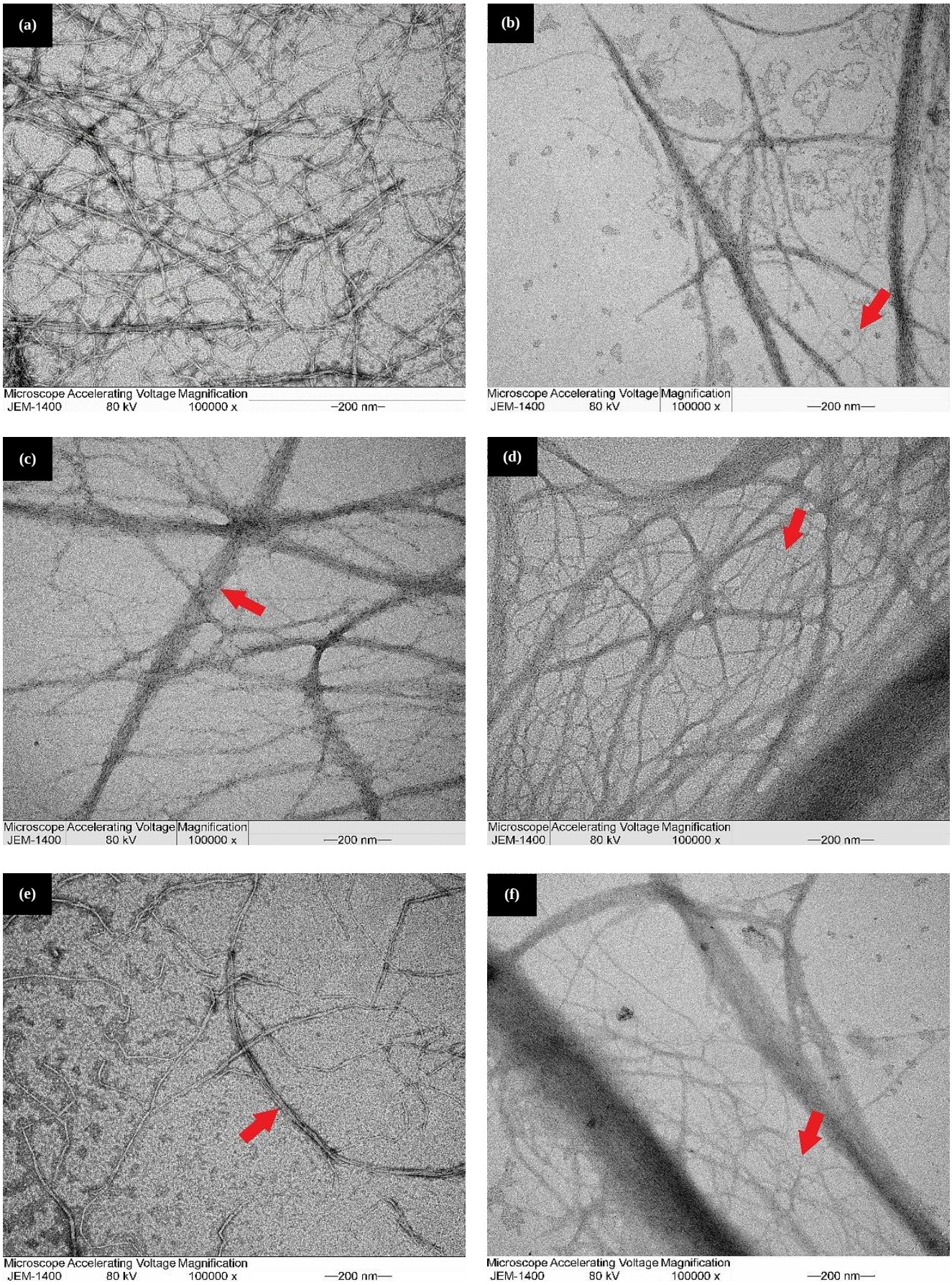

Figure 5. TEM images at 100,000× magnification of the CNFs: (a, b) 0.5%, (c, d) 0.7% and (e, f) 1.0%, for defibrillation time of 30 min and 60 min, respectively.

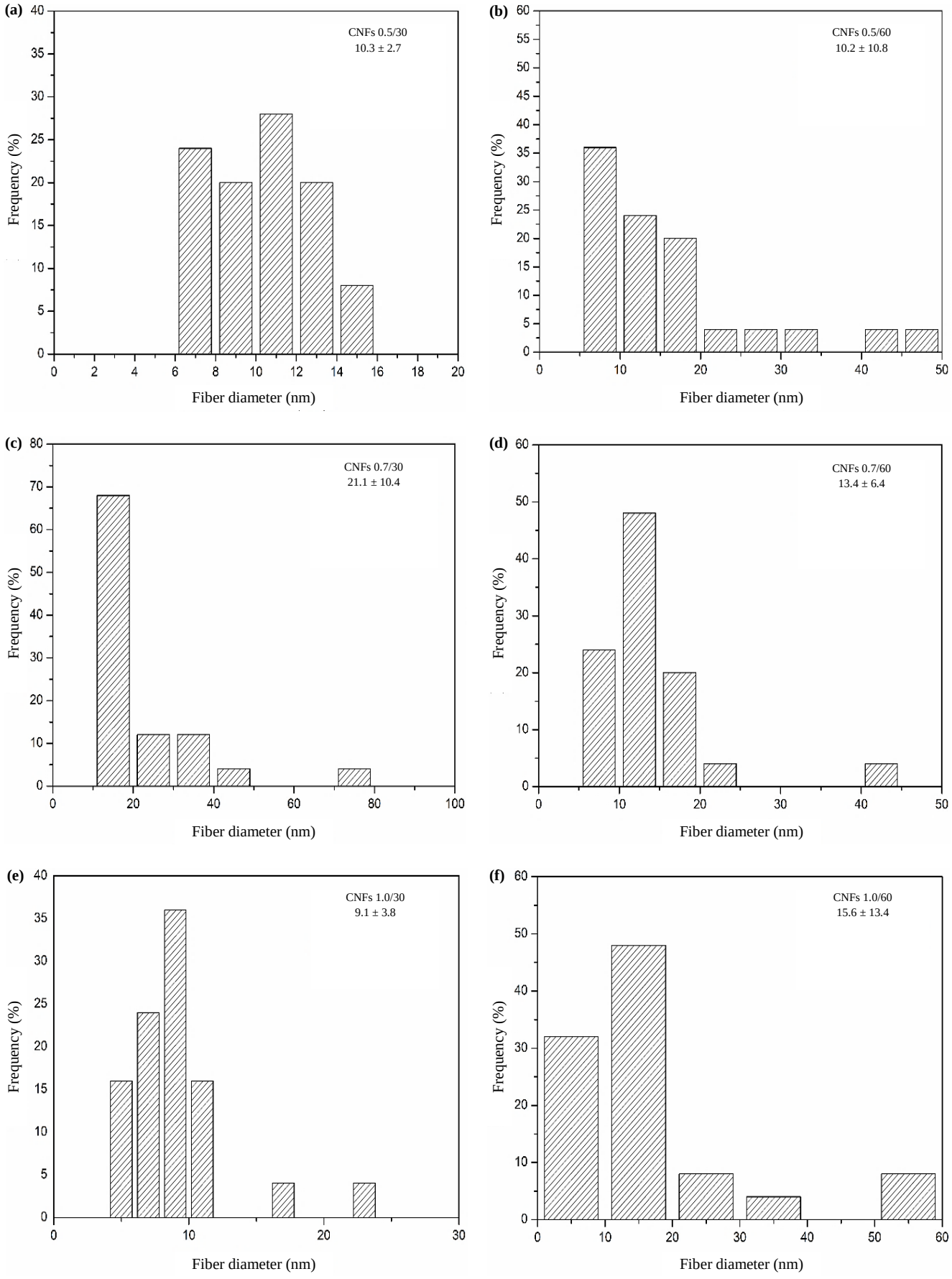

Figure 6. Fiber diameter distribution histograms of the CNFs: (a, b) 0.5%, (c, d) 0.7% and (e, f) 1.0%, for defibrillation time of 30 min and 60 min, respectively.

3.4 Optical transmittance

As clearly seen in Figure 7, the prepared CNFs after passing through high-pressure homogenization exhibited a gel-like structure. Figure 8 gives UV–vis transmittance spectra of CNFs prepared at different conditions. For each fiber concentration, 60 min of defibrillation times gave more transparent appearance as compared to 30 min of defibrillation time. It can be seen that higher percentage of transmittance was achieved for the fiber suspension produced at 60 min of defibrillation time, as compared to those prepared at 30 min of defibrillation time. This result is similar to previous report that suggesting prolonged defibrillation time led to transparent suspension [14]. One possible explanation for the transparency is the smaller fibril diameter obtained at longer period of defibrillation [28,29].

3.5 Thermogravimetric analysis

TGA and DTG curves for all samples are graphically represented in Figure 9. All samples gave an initial weigh loss below 150°C due to the evaporation of loosely bound moisture on the surface of the samples [30]. Interestingly, it was observed that the DTG curve of raw fibers contained two peaks (T_{peak} = 292°C and 358°C). The first peak ranging from 265°C to 317°C was due to the thermal depolymerization of hemicellulose, while the second degradation stage was from 325°C to 389°C, attributed to the degradation of cellulose [31]. A likely explanation is that the raw fibers did not undergo any chemical treatment, making it contain high amount of hemicellulose, lignin, and non-cellulosic substances, which triggered degradation at lower temperature [32].

As for purified fibers, a narrower range of decomposition was observed from 305°C to 383°C. The single peak of purified fibers in DTG curve was accounted for efficient removal of lignin and hemicellulose in chemical treatment. In addition, the onset of degradation temperature of purified fibers was shifted to a higher value as compared to raw fibers from 265°C to 326°C. This observation indicated the effectiveness of lignin and hemicellulose removal during chemical treatment, which is in accordance with FTIR analysis and chemical composition result as well.

The TGA and DTG curves of purified fibers and CNFs followed the same trend, also exhibited a single decomposition stage. However, a minor difference was a relatively lower thermal stability for CNFs, although both were having the same chemical composition. The lower thermal stability of CNFs could be an implication of its smaller dimension than purified fibers, resulting in the higher specific surface area [10]. With the highly fibrillated structure and smaller dimensions, CNFs were more vulnerable to degrade under same heating condition [21]. There was no significant change on the thermal behaviour of CNFs by varying the fiber concentration and defibrillation time, with the onset of degradation temperature ranged 302°C to 306°C. This phenomenon can be explained by the same chemical treatment method applied for all CNFs samples and their thermal characteristics were not affected by the defibrillation time used in this research.

Figure 7. Appearance of aqueous suspensions of CNFs with fiber concentration 0.5, 0.7, 1.0%w/v and defibrillation time 30 min and 60 min.

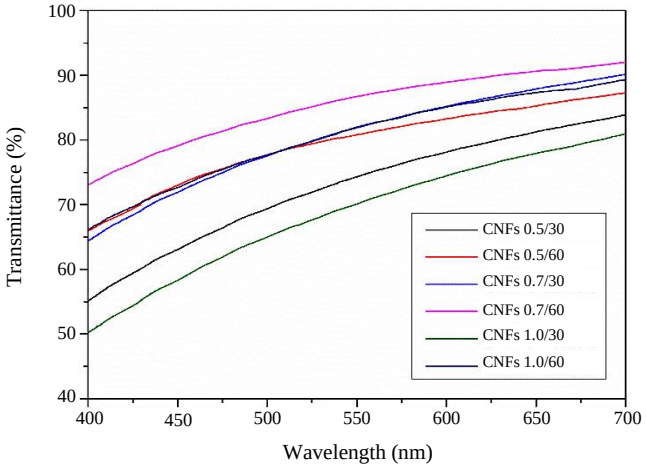

Figure 8. Transmittance of 0.1% suspensions of CNFs with fiber concentration 0.5, 0.7, and 1.0%w/v and defibrillation time 30 min and 60 min.

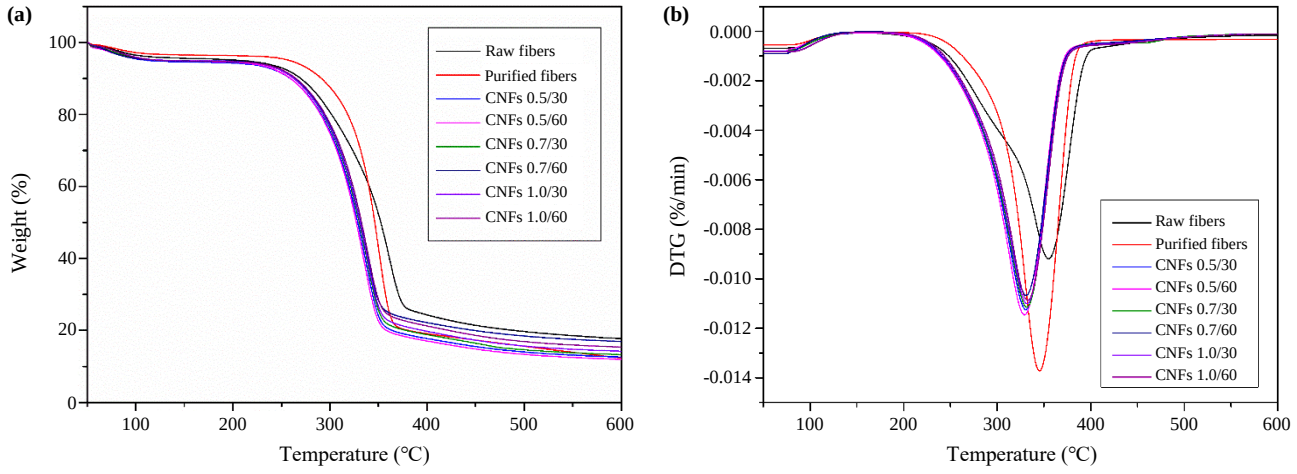

Figure 9. (a) TG and (b) first derivative TG (DTG) curves of the raw fibers, purified fibers and CNFs.

3.5 Degree of crystallinity

As presented in Figure 10, the cellulose XRD diffraction patterns were recorded at 2θ = 15.7° and 22.6°, which are the characteristic peaks of cellulose corresponding to the lattice planes 110 and 200 [33]. An increase of CI was seen for purified fibers as compared to raw fibers from 47.4% to 71.45%, which were similar value with those estimated by Azrina *et al*. [34] and Lani *et al*. [35] using the same raw material. This finding can be explained by the elimination of amorphous portion of the purified fibers, contributed by hemicellulose and lignin [36], which is corresponding to FTIR and chemical composition analysis.

The CI value for CNFs was found to be in the range of 64.33% to 65.98%, which was slightly lower than purified fibers. This was probably due to the high shear force experienced by CNFs in high-pressure homogenizer that can affect their crystal structure. The damage of crystalline domains of CNFs by homogenizer was also reported in the previous research [37,38].

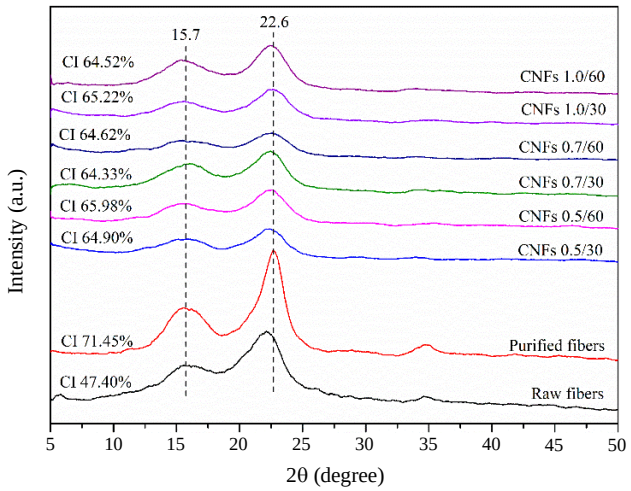

Figure 10. XRD spectra of raw fibers, purified fibers and CNFs.

4. Conclusions

In this study, CNFs were successfully extracted from EPFB using chemical treatment and high-pressure homogenization. The chemical composition and FTIR analysis strongly confirmed the effective removal of hemicellulose and lignin by chemical treatment, supported by the SEM images that showed surface changes of fibers from rough to smooth surface. Moreover, FE-SEM and TEM images showed that nano-sized cellulose fibers with diameter 6-16 nm were obtained. By varying fiber concentration and defibrillation time of CNFs, different morphologies were observed. Fiber concentration of 0.5% recorded the best uniformity of diameter size, while higher number of fine fiber branches were seen for longer defibrillation time of 60 min. Additionally, CNFs were found to obtain similar thermal degradation behaviour and crystalline structure as purified fibers. However, CNFs degraded at slightly lower temperature than purified fibers and had lower CI value than purified fibers as an influence from the mechanical forces encountered by CNFs in high-pressure homogenization. In short, the obtained nanofibers from EPFB could be used in various applications such as packaging films, reinforcing filler, as well as medical applications.

Acknowledgements

The research was made possible by support from ASEAN University Network/Southeast Asia Engineering Education Development Network (AUN/SEED-net) for providing GAICCE DDP Scholarship.

References

[1] F.H. Isikgor, and C.R. Becer, "Lignocellulosic biomass: a sustainable platform for the production of bio-based chemicals and polymers," *Polymer Chemistry*, vol. 6, no. 25, pp. 4497-4559, 2015.

[2] A. Barhoum, H. Li, M. Chen, L. Cheng, W. Yang, and A. Dufresne, "Emerging applications of cellulose nanofibers," in *Handbook of Nanofibers*, 2019, pp. 1131-1156.

[3] A. Blanco, M.C. Monte, C. Campano, A. Balea, N. Merayo, and C. Negro, "Nanocellulose for industrial use," in *Handbook of Nanomaterials for Industrial Applications*, 2018, pp. 74-126.

[4] J. Huang, X. Ma, G. Yang, and A. Dufresne, "Introduction to nanocellulose," in *Nanocellulose: From Fundamentals to Advanced Materials*, Jin Huang, A. Dufresne, and N. Lin Eds.: Wiley-VCH Verlag GmbH & Co. KGaA, 2019, pp. 1-20.

[5] M.F. Awalludin, O. Sulaiman, R. Hashim, and W.N.A.W. Nadhari, "An overview of the oil palm industry in Malaysia and its waste utilization through thermochemical conversion, specifically via liquefaction," *Renewable and Sustainable Energy Reviews*, vol. 50, pp. 1469-1484, 2015.

[6] P. Wadchasit, C. Siripattana, and K. Nuithitikul, "The effect of pretreatment methods for improved biogas production from oil-palm empty fruit bunches (EFB)," *IOP Conference Series: Earth and Environmental Science*, vol. 463, no. 1, pp. 8-14, 2020.

[7] Y. Okahisa, Y. Furukawa, K. Ishimoto, C. Narita, K. Intharapichai, and H. Ohara, "Comparison of cellulose nanofiber properties produced from different parts of the oil palm tree," *Carbohydrate Polymers*, vol. 198, pp. 313-319, 2018.

[8] A. Ferrer, I. Filpponen, A. Rodriguez, J. Laine, and O.J. Rojas, "Valorization of residual empty palm fruit bunch fibers (EPFBF) by microfluidization: production of nanofibrillated cellulose and EPFBF nanopaper," *Bioresource Technology*, vol. 125, pp. 249-55, 2012.

[9] S. Gea, A.H. Siregar, E. Zaidar, M. Harahap, D.P. Indrawan, and Y.A. Perangin-Angin, "Isolation and characterisation of cellulose nanofibre and lignin from oil palm empty fruit bunches," *Materials*, vol. 13, no. 10, pp. 2290, 2020.

[10] I.P. Mahendra, B. Wirjosentono, Tamrin, H. Ismail, and J.A. Mendez, "Thermal and morphology properties of cellulose nanofiber from TEMPO-oxidized lower part of empty fruit bunches (LEFB)," *Open Chemistry*, vol. 17, no. 1, pp. 526-536, 2019.

[11] M. Jonoobi, A. Khazaeian, P.M. Tahir, S.S. Azry, and K. Oksman, "Characteristics of cellulose nanofibers isolated from rubberwood and empty fruit bunches of oil palm using chemo-mechanical process," *Cellulose*, vol. 18, no. 4, pp. 1085-1095, 2011.

[12] M.A.F. Supian, K.N.M. Amin, S.S. Jamari, and S. Mohamad, "Production of cellulose nanofiber (CNF) from empty fruit bunch (EFB) via mechanical method," *Journal of Environmental Chemical Engineering*, vol. 8, no. 1, 2020.

[13] A. Kadimi, K. Benhamou, Y. Habibi, Z. Ounaies, and H. Kaddami, "Nanocellulose alignment and electrical properties improvement," in *Multifunctional Polymeric Nanocomposites Based on Cellulosic Reinforcements*, D. Puglia, E. Fortunati, and J.M. Kenny, Elsevier, 2016, pp. 343-376.

[14] K. Pacaphol, and D. Aht-Ong, "Preparation of hemp nanofibers from agricultural waste by mechanical defibrillation in water," *Journal of Cleaner Production*, vol. 142, pp. 1283-1295, 2017.

[15] H.K. Goering, and P.J.V. Soest, *Forage Fiber Analyses (Apparatus, Reagents, Procedures, and Some Applications)*. Washington, D.C.: Agricultural Research Service, United States Department of Agriculture, 1970.

[16] L. Segal, J.J. Creely, A.E. Martin, and C.M. Conrad, "An empirical method for estimating the degree of crystallinity of native cellulose using the X-ray diffractometer," *Textile Research Journal*, vol. 29, no. 10, pp. 786-794, 1959.

[17] H.V. Lee, S.B. Hamid, and S.K. Zain, "Conversion of lignocellulosic biomass to nanocellulose: structure and chemical process," *The Scientific World Journal*, vol. 2014, pp. 631013, 2014.

[18] V. Oriez, J. Peydecastaing, and P.-Y. Pontalier, "Lignocellulosic biomass mild alkaline fractionation and resulting extract purification processes: conditions, yields, and purities," *Clean Technologies*, vol. 2, no. 1, pp. 91-115, 2020.

[19] X. Miao, J. Lin, and F. Bian, "Utilization of discarded crop straw to produce cellulose nanofibrils and their assemblies," *Journal of Bioresources and Bioproducts*, vol. 5, no. 1, pp. 26-36, 2020.

[20] P. Panyasiri, N. Yingkamhaeng, N.T. Lam, and P. Sukyai, "Extraction of cellulose nanofibrils from amylase-treated cassava bagasse using high-pressure homogenization," *Cellulose*, vol. 25, no. 3, pp. 1757-1768, 2018.

[21] J. Wu, X. Du, Z. Yin, S. Xu, S. Xu, and Y. Zhang, "Preparation and characterization of cellulose nanofibrils from coconut coir fibers and their reinforcements in biodegradable composite films," *Carbohydrate Polymers*, vol. 211, pp. 49-56, 2019.

[22] A.d.S. Fonseca, S. Panthapulakka, S.K. Konar, M. Sain, L. Bufalinof, J. Raabe, I.P.d.A. Miranda, M.A. Martins, and G.H.D. Tonoli, "Improving cellulose nanofibrillation of non-wood fiber using alkaline and bleaching pre-treatments," *Industrial Crops and Products*, vol. 131, pp. 203-212, 2019.

[23] I. Hongrattanavichit, and D. Aht-Ong, "Nanofibrillation and characterization of sugarcane bagasse agro-waste using water-based steam explosion and high-pressure homogenization," *Journal of Cleaner Production*, vol. 277, pp. 123471, 2020.

[24] F. Xu, J. Yu, T. Tesso, F. Dowell, and D. Wang, "Qualitative and quantitative analysis of lignocellulosic biomass using infrared techniques: A mini-review," *Applied Energy*, vol. 104, pp. 801-809, 2013.

[25] K. Pakutsah, and D. Aht-Ong, "Facile isolation of cellulose nanofibers from water hyacinth using water-based mechanical defibrillation: Insights into morphological, physical, and rheological properties," *International Journal of Biological Macromolecules*, vol. 145, pp. 64-76, 2020.

[26] H. Chen, Y. Yu, T. Zhong, Y. Wu, Y. Li, Z. Wu, and B. Fei "Effect of alkali treatment on microstructure and mechanical properties of individual bamboo fibers," *Cellulose*, vol. 24, no. 1, pp. 333-347, 2017.

[27] B. Kumar, N. Bhardwaj, K. Agrawal, V. Chaturvedi, and P. Verma, "Current perspective on pretreatment technologies using lignocellulosic biomass: An emerging biorefinery concept," *Fuel Processing Technology*, vol. 199, 2020.

[28] F. Jiang, S. Han, and Y.-L. Hsieh, "Controlled defibrillation of rice straw cellulose and self-assembly of cellulose nanofibrils into highly crystalline fibrous materials," *RSC Advances*, vol. 3, pp. 12366-12375, 2013.

[29] V. Kumar, V. Ottesen, K. Syverud, Ø.W. Gregersen, and M. Toivakka, "Coatability of Cellulose Nanofibril Suspensions: Role of Rheology and Water Retention," *BioResources*, vol. 12, no. 4, pp. 7656-7679, 2017.

[30] K.Y. Goh, Y.C. Ching, C.H. Chuah, L.C. Abdullah, and N.-S. Liou, "Individualization of microfibrillated celluloses from oil palm empty fruit bunch: comparative studies between acid hydrolysis and ammonium persulfate oxidation," *Cellulose*, vol. 23, no. 1, pp. 379-390, 2015.

[31] H. Yang, R. Yan, H. Chen, D.H. Lee, and C. Zheng, "Characteristics of hemicellulose, cellulose and lignin pyrolysis," *Fuel*, vol. 86, no. 12-13, pp. 1781-1788, 2007.

[32] W. Yang, Y. Feng, H. He, and Z. Yang, "Environmentally-friendly extraction of cellulose nanofibers from steam-explosion pretreated sugar beet pulp," *Materials*, vol. 11, no. 7, pp. 1160, 2018.

[33] C. Trilokesh, and K.B. Uppuluri, "Isolation and characterization of cellulose nanocrystals from jackfruit peel," *Scientific Reports*, vol. 9, no. 1, pp. 16709, 2019.

[34] Z.A. Zianor Azrina, M.D.H. Beg, M.Y. Rosli, R. Ramli, N. Junadi, and A. Alam, "Spherical nanocrystalline cellulose (NCC) from oil palm empty fruit bunch pulp via ultrasound assisted hydrolysis," *Carbohydrate Polymers*, vol. 162, pp. 115-120, 2017.

[35] N.S. Lani, N. Ngadi, A. Johari, and M. Jusoh, "Isolation, characterization, and application of nanocellulose from oil palm empty fruit bunch fiber as nanocomposites," *Journal of Nanomaterials*, vol. 2014, pp. 1-9, 2014.

[36] A. Zoghlami, and G. Paes, "Lignocellulosic biomass: Understanding recalcitrance and predicting hydrolysis," *Frontiers in Chemistry*, vol. 7, pp. 874, 2019.

[37] H. Du, C. Liu, Y. Zhang, G. Yu, C. Si, and B. Li, "Preparation and characterization of functional cellulose nanofibrils via formic acid hydrolysis pretreatment and the followed high-pressure homogenization," *Industrial Crops and Products*, vol. 94, pp. 736-745, 2016.

[38] K. Saelee, N. Yingkamhaeng, T. Nimchua, and P. Sukyai, "An environmentally friendly xylanase-assisted pretreatment for cellulose nanofibrils isolation from sugarcane bagasse by high-pressure homogenization," *Industrial Crops and Products*, vol. 82, pp. 149-160, 2016.